

11-8-2004

Modified Quantum Trajectory Dynamics Using a Mixed Wave Function Representation

Sophya Garashchuk

University of South Carolina--Columbia, sgarashc@chem.sc.edu

Vitaly A. Rassolov

University of South Carolina - Columbia, rassolov@chem.sc.edu

Follow this and additional works at: https://scholarcommons.sc.edu/chem_facpub



Part of the [Chemistry Commons](#)

Publication Info

Published in *Journal of Chemical Physics*, Volume 121, Issue 18, 2004, pages 8711-

© [Journal of Chemical Physics](#) 2004, American Institute of Physics.

This Article is brought to you by the Chemistry and Biochemistry, Department of at Scholar Commons. It has been accepted for inclusion in Faculty Publications by an authorized administrator of Scholar Commons. For more information, please contact digres@mailbox.sc.edu.

Modified quantum trajectory dynamics using a mixed wave function representation

Sophya Garashchuk and Vitaly A. Rassolov

Department of Chemistry and Biochemistry, University of South Carolina, South Carolina 29208

(Received 10 August 2004; accepted 16 August 2004)

Dynamics of quantum trajectories provides an efficient framework for description of various quantum effects in large systems, but it is unstable near the wave function density nodes where the quantum potential becomes singular. A mixed coordinate space/polar representation of the wave function is used to circumvent this problem. The resulting modified trajectory dynamics associated with the polar representation is nonsingular and smooth. The interference structure and the nodes of the wave function density are described, in principle, exactly in the coordinate representation. The approximate version of this approach is consistent with the semiclassical linearized quantum force method [S. Garashchuk and V. A. Rassolov, *J. Chem. Phys.* **120**, 1181 (2004)]. This approach is exact for general wave functions with the density nodes in a locally quadratic potential. © 2004 American Institute of Physics. [DOI: 10.1063/1.1804177]

I. INTRODUCTION

Recently, the hydrodynamic or the de Broglie–Bohm formulation of the Schrödinger equation (SE) (Ref. 1) has gained attention as an alternative approach to solving the time-dependent SE. In principle, this formulation which is based on the polar representation of the wave function can give an efficient description of quantum effects in large molecular systems with the linear scaling with respect to the system size, in contrast to the exponential scaling of the exact methods of quantum dynamics. In the context of nuclear dynamics the conceptual appeal of this formulation is that, formally, quantum potential vanishes in the $\hbar \rightarrow 0$ limit (or in the large mass limit) appropriate for description of heavy particles such as nuclei.

The formalism, outlined below in one dimension for a particle of mass m , is based on the substitution of a wave function in terms of its real amplitude and phase

$$\psi(x,t) = A(x,t) \exp\left(\frac{i}{\hbar} S(x,t)\right) \quad (1)$$

into SE, which gives the Hamilton-Jacobi equation on the wave function phase $S(x,t)$,

$$\frac{\partial S(x,t)}{\partial t} + \frac{[S'(x,t)]^2}{2m} + V + U = 0, \quad (2)$$

and the equation on the wave function amplitude

$$\frac{\partial A(x,t)}{\partial t} + A'(x,t) \frac{S'(x,t)}{m} + \frac{A(x,t)}{2m} S''(x,t) = 0. \quad (3)$$

The latter expresses the continuity of the wave function density. The prime denotes differentiation with respect to x . The gradient of the phase is associated with the momentum of a trajectory, $S'(x,t) = p(x,t)$, which evolves in time according to the Hamilton's equations of motion in the presence of the classical potential V and the quantum potential U ,

$$U = -\frac{\hbar^2}{2m} \frac{A''(x,t)}{A(x,t)}. \quad (4)$$

In the Lagrangian frame of reference Eqs. (2) and (3) become local with respect to $p(x,t)$, once the latter is expressed in terms of a trajectory weight $w(x,t)$ as $dw(x,t)/dt = 0$.² The trajectory weight is the amount of density within a volume element δx_t associated with each trajectory, $w(x,t) = A^2(x,t) \delta x_t$. The quantum effects enter the formulation via a *single nonlocal* object—the quantum potential U —at the expense of giving up the linearity of the standard SE. The quantum trajectories serve as a useful visualization tool^{3,4} and the formalism has also been adapted for cases of nonadiabatic dynamics^{5,6} phase-space representations and density matrix approaches.^{7–13} From the computational standpoint the appeal of this formulation is that Eq. (2) can provide an ultimate sparse moving grid, since $A(x,t)$ and $S(x,t)$ are often slowly varying functions compared to the complex $\psi(x,t)$, and the trajectory weights are conserved in a closed system. Several numerical strategies based on the local interpolation of the wave function density were suggested^{14–18} and some of them proved to be efficient for model problems (scattering and dissociation) in many dimensions. For general problems, however, accurate numerical implementation of the quantum trajectory formulation is hindered by the special features of quantum trajectory dynamics: (i) quantum trajectories cannot cross and (ii) the quantum potential becomes singular when the density of the wave function vanishes. These properties lead to complicated and rapidly varying in time and space quantum potentials and to quantum forces that are very difficult to compute accurately. The accuracy of the quantum potential and, consequently, the stability and accuracy of dynamics was found to deteriorate with time, especially in the presence of the density nodes, which motivated the development of the representation

transformation, adaptive moving grids, artificial viscosity techniques, covering functions, and wave function decomposition.^{19–23}

The quantum trajectory formalism has also been used as a starting point for approximate local methods based on expansion around individual trajectories, such as the derivative propagation method²⁴ and the method utilizing trajectory stability properties.²⁵ We use the quantum trajectory framework as a basis for a semiclassical method using the concept of the *approximate* quantum potential determined from the ensemble of trajectories with well-defined classical and quantum-mechanical limits.^{2,26,27} While the implementation of these approximate/semiclassical methods is formally insensitive to the presence of the wave function nodes, it is desirable to have an efficient and accurate description of general wave functions, including excited states, interference and tunneling effects. Below we demonstrate that a mixed coordinate space/polar representation of the wave function defines smooth nonsingular trajectory dynamics, reflecting the overall behavior of the system, while more local features due to interference or initial conditions are accurately described by the coordinate space part.

II. THE MIXED REPRESENTATION APPROACH

First let us illustrate the instability problem of the exact Bohmian dynamics in the regions of the low wave function density. The polar representation of a wave function, Eq. (1), leads to a singular quantum potential near the node where $A(x,t)=0$. This results in the large quantum force, rapid changes in the momentum and “jumps” in the phase of the Bohmian trajectories as they move around the node. The time propagation becomes very expensive even if the quantum potential is provided, and nearly impossible with approximate methods. Figure 1 shows quantum trajectories describing the time evolution of a wave function defined at $t=0$ as a superposition of the zeroth and the first coherent states of the harmonic oscillator²⁸ under the influence of the Hamiltonian $H=\hat{p}^2/2+w^2x^2/2$ with the frequency $w=2$. The wave function density exhibits a single minimum at $t=0$ which develops into a node around times $t=\{1.0,2.5,4.0\}$, when the quantum forces become very large. Around these times the initially equidistant trajectories closely approach each other as the wave function density minimum decreases. The trajectory momenta in the nodal region grow rapidly and reverse their direction after this minimum reaches zero. The range of the momenta for trajectories in the nodal regions and on the tails of the wave function can differ by orders of magnitude, depending on how close a trajectory is to the node. In contrast, the wave function in its complex form remains smooth and simply changes sign at the node. For general systems, the pattern of the node development in the course of interference is the same. The only exception to this picture, which is beyond the scope of semiclassical dynamics, are the nodes of excited eigenstates, for which singularities in the quantum potential cancel exactly, the density is stationary and the trajectories have zero momenta. In general, an efficient description of the nodes

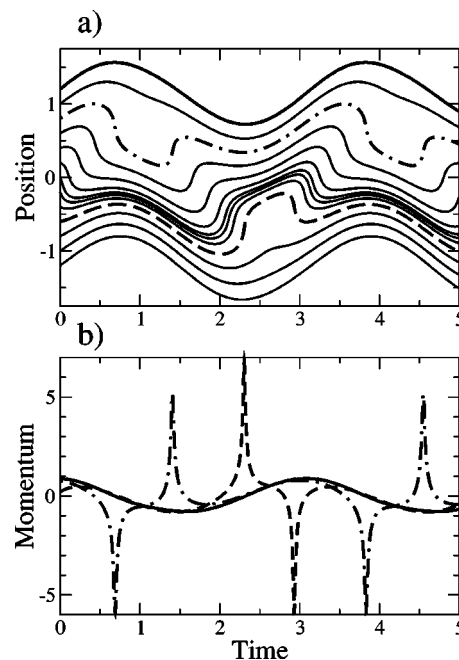


FIG. 1. Bohmian dynamics in the presence of the density nodes: (a) position of the trajectories as a function of time; (b) momenta for three selected trajectories shown with the thick, dashed, and dot-dashed lines on both panels. Results are shown in atomic units.

and interference pattern based on stable nonsingular trajectory dynamics reflecting the physics of the system is clearly desirable.

This can be achieved by using a new representation of the wave function. We allow the amplitude $A(x,t)$ to become complex and represent $\psi(x,t)$ as

$$\psi(x,t) = a(x,t)\chi(x,t)\exp\left(\frac{i}{\hbar}s(x,t)\right) \quad (5)$$

instead of Eq. (1), which is valid if zeros of $A(x,t)$ and $\chi(x,t)$ coincide. Function $\chi(x,t)$ is in general complex and is chosen to make the new real amplitude $a(x,t)$ and phase $s(x,t)$ smooth. Substitution of Eq. (5) into SE and separation of the real and imaginary parts give

$$\frac{\partial s(x,t)}{\partial t} + \frac{s'(x,t)^2}{2m} + V - \frac{\hbar^2}{2m} \frac{a''(x,t)}{a(x,t)} + \hbar \operatorname{Im} \left[\frac{W}{\chi(x,t)} \right] = 0, \quad (6)$$

$$\begin{aligned} \frac{\partial a(x,t)}{\partial t} + \frac{s'(x,t)}{m} a'(x,t) + \frac{s''(x,t)}{2m} a(x,t) \\ + a(x,t) \operatorname{Re} \left[\frac{W}{\chi(x,t)} \right] = 0, \end{aligned} \quad (7)$$

where terms dependent on $\chi(x,t)$ are collected in a function W ,

$$\begin{aligned} W = \frac{\partial \chi(x,t)}{\partial t} + \frac{s'(x,t)}{m} \chi'(x,t) \\ - \frac{i\hbar}{m} \left(\frac{\chi''(x,t)}{2} + \frac{a'(x,t)}{a(x,t)} \chi'(x,t) \right). \end{aligned} \quad (8)$$

Symbols $\text{Re}[\dots]$ and $\text{Im}[\dots]$ denote real and imaginary parts of a quantity. Now, treating Eq. (6) as the Hamilton-Jacobi equation and identifying $s'(x,t)$ with the no-longer-Bohmian trajectory momentum, $s'(x,t)=p(x,t)$, in the Lagrangian frame of reference we obtain Bohmian-like equations for $s(x,t)$ and $a(x,t)$ using a *partial* quantum potential U_a ,

$$U_a = -\frac{\hbar^2}{2m} \frac{a''(x,t)}{a(x,t)}. \quad (9)$$

Equation (6) becomes

$$\frac{ds(x,t)}{dt} = \frac{p^2(x,t)}{2m} - \left(V + U_a + \hbar \text{Im} \left[\frac{W}{\chi(x,t)} \right] \right). \quad (10)$$

Equation (7) can be expressed in terms of the partial trajectory weights, $w_a(x,t)=a^2(x,t)\delta x_t$, as

$$\frac{dw_a(x,t)}{dt} = -2w_a(x,t) \text{Re} \left[\frac{W}{\chi(x,t)} \right]. \quad (11)$$

Ideally, $\chi(x,t)$ is determined by setting $W=0$. Then, Eqs (10) and (11) become fully analogous to the Bohmian equations (2) and (3): in a closed system the new weights $w_a(x,t)$ along the modified quantum trajectories are conserved, the partial quantum potential U_a is finite and the nodes are described by the function $\chi(x,t)$. The new trajectories reflect the overall behavior of the wave function and, therefore, give a compact representation of dynamics. For an exact implementation $\chi(x,t)$ can be represented in a complete basis with the expansion coefficients determined variationally similar to the procedure of Ref. 29.

Let us apply the new mixed representation approach to the harmonic oscillator example discussed above. The Hamiltonian in atomic units is $H=\hat{p}^2/m/2+w^2x^2/2$ with the parameter values $m=1$ and $w=2$. The initial wave packet is a Gaussian multiplied by a complex linear function

$$\psi(x,0) = \left(\frac{2\alpha}{\pi} \right)^{1/4} \frac{k \exp(i\kappa) + 2\sqrt{\alpha}(x-x_0)}{\sqrt{1+k^2}} \times \exp[-\alpha(x-x_0)^2 + i p_0(x-x_0)]. \quad (12)$$

In this case $p(x,t)$ and $r(x,t)=a'(x,t)/a(x,t)$ are linear functions of x for all times, and linear $\chi(x,t)$,

$$\chi(x,t) = \chi_0(t) + \chi_1(t)x, \quad (13)$$

solves $W=0$ which takes the following form

$$\partial \chi(x,t) / \partial t = -[p(x,t) - i\hbar r(x,t)] \chi'(x,t) / m. \quad (14)$$

Equations (13) and (14) define the time dependence of $\chi_0(t)$ and $\chi_1(t)$. These expressions are integrated numerically with parameters of linear $p(x,t)$ and $r(x,t)$ coming from the global least square fit; $r(x,t)$ also defines the partial quantum potential U_a of Eq. (6) needed to propagate the trajectories as described in Ref. 27. Results for the coherent wave packet with the initial parameters $\{\alpha=1, x_0=0, p_0=1, k=0.5, \kappa=\pi/3\}$ are shown on Figs. 2(a)–2(b). Dynamics of the new trajectories is smooth and describes the oscillatory behavior of the polar part of the wave function, while $\chi(x,t)$ describes the evolution of the density minimum which passes through the node twice (compare the trajectories to those of Fig. 1).

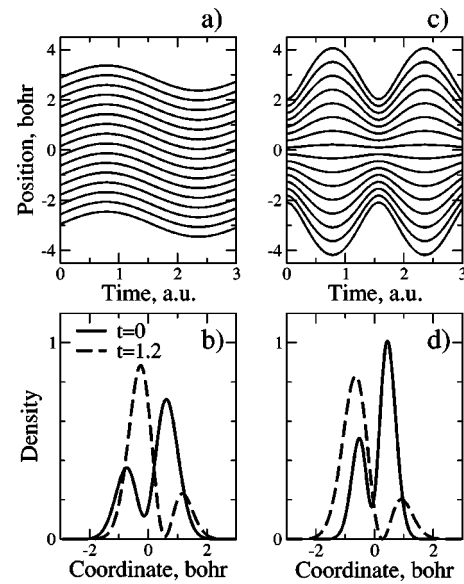


FIG. 2. The mixed representation dynamics of a coherent wave packet in a quadratic potential: modified trajectories as a function of time (a) and the wave function density (b). Dynamics of a noncoherent wave packet: modified trajectories (c) and the wave function density (d). The legend for the panel (d) is the same as on the panel (b).

Figure 2(b) shows the initial wave function density and the density with the node at a later time. For the noncoherent initial wave function with initial parameters $\{\alpha=2, x_0=0, p_0=0, k=0.5, \kappa=\pi/3\}$ the new trajectories describe the spreading and contraction of the Gaussian “envelope” function, while $\chi(x,t)$ represents the internal structure of $\psi(x,t)$ as shown on Figs. 2(c)–2(d). The numerical implementation of the modified quantum trajectory dynamics is orders of magnitude cheaper than the cost of the Bohmian dynamics even with the full quantum potential U being available in analytical form for this system.

III. THE LINEARIZED IMPLEMENTATION

For general potentials the wave function nodes will develop in the process of interference for any initial wave function. In order to describe this behavior we will have to introduce the mixed representation in the course of dynamics. In line with the approximate quantum potential approach geared toward large semiclassical systems, we will determine $\chi(x,t)$ approximately. In Refs. 27 and 30 we define the energy-conserving approximate quantum potential based on the linearization of the nonclassical component of the momentum operator, $r(x,t)=A'(x,t)/A(x,t)$, which produces linearized quantum force (LQF). The optimal LQF parameters $\{a_0, a_1\}$ minimize a functional $I = \int [r(x,t) - a_0 - a_1 x]^2 A^2(x,t) dx$. After the trajectory discretization the LQF parameters are found in terms of the first and second moments of the trajectory distribution. In the mixed representation we can define an approximate partial quantum potential U_a in a similar way, now using $r(x,t)=a'(x,t)/a(x,t)$ as the nonclassical momentum and the full wave function density $|\psi(x,t)|^2 = a(x,t)^2 |\chi(x,t)|^2$ as a weighting function in the optimization procedure. The function $\chi(x,t)$ is taken to be linear (which is sufficiently accurate in the vicinity of a node), and

it is defined in such a way that all χ -dependent terms in Eq. (10) cancel provided that the linearized nonclassical momentum, $\tilde{r}(x,t)$ is used throughout. The parameters of $\chi(x,t)$ will satisfy

$$\frac{\partial \chi(x,t)}{\partial t} = -\frac{1}{m} [\tilde{p}(x,t) - i\hbar \tilde{r}(x,t)] \chi'(x,t). \quad (15)$$

Function $\tilde{p}(x,t)$ is the linearized component of the momentum operator found as the least square fit to $p(x,t)$ weighted by the wave function density. With the linear $\chi(x,t)$, given by Eq. (13) and satisfying Eq. (15), Eq. (11) for the trajectory weights can be written as

$$\frac{dw_a(x,t)}{dt} = -\frac{2w_a(x,t)}{m} (W_r + W_i), \quad (16)$$

where

$$W_r = \text{Re}[\chi^{-1}(x,t)\chi_1(t)][p(x,t) - \tilde{p}(x,t)], \quad (17)$$

$$W_i = \hbar \text{Im}[\chi^{-1}(x,t)\chi_1(t)][r(x,t) - \tilde{r}(x,t)]. \quad (18)$$

Equation (16) cannot be solved exactly along a trajectory since W_i includes a nonlocal term $r(x,t)$, but the contribution of W_i can be evaluated in average using integration by parts. The final equation for the j th trajectory weight is

$$\begin{aligned} \frac{dw_a(x_j,t)}{dt} = & -\frac{2w_a(x_j,t)}{m} \left(W_r - \hbar \text{Im}[\chi_0^*(t)\chi_1(t)] \right. \\ & \left. \times \sum_i \tilde{r}(x_i,t)w_a(x_i,t) \right). \end{aligned} \quad (19)$$

The total normalization of the wave function is strictly conserved.

In general, the accuracy of this description will depend on adjustment of the balance between the polar and coordinate space representation of a wave function in the course of dynamics. For example, in the context of the LQF method for a wave function which is a Gaussian at $t=0$, a constant $\chi(x,t)$ will be adequate at short times. At a later time the linear $\chi(x,t)$ will be introduced to improve the accuracy. Its parameters can be defined from the minimization of a functional

$$I = \int \left| \frac{\psi'(x,t)}{\psi(x,t)} - g(x) - \frac{1}{z+x} \right|^2 a^2(x,t) dx, \quad (20)$$

where $g(x) = a_0 + a_1 x$ is a complex linear function approximating the linear part of the momentum operator components $r(x,t)$ and $p(x,t)$, with respect to complex parameters $\{a_0, a_1, z\}$. Once optimal z , which is zero of $\chi(x,t)$ in the complex plane, is known the function $\chi(x,t)$ is obtained from $\chi'(x,t)/\chi(x,t) = 1/(x+z)$. As in the LQF method the minimization procedure, once discretized over the trajectories is expressed in terms of the moments of x and p and is linear with respect to $\{a_0, a_1\}$. The only nonlinear part requiring iterative solution is optimization of z . Once parameters of $\chi(x,t)$ are determined new weights $w_a(x,t)$, momenta $p(x,t)$ and phases $s(x,t)$ for the trajectories are found by equating the wave function in the old, in this case polar representation given by Eq. (1), with the new mixed representation given by Eq. (5). For improved description the pro-

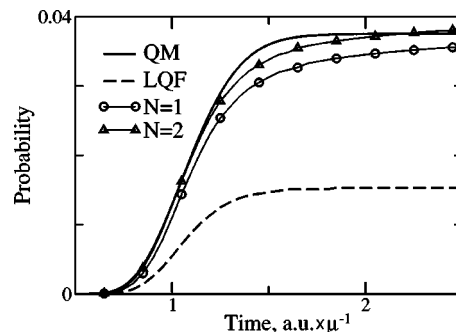


FIG. 3. The wave packet transmission probability for the Eckart barrier as a function of time. The LQF result is shown with the dashed line, the quantum result is shown with the solid line. The mixed representation results with $\chi(x,t)$ introduced at $t=0.1$ and with an additional reexpansion at $t=0.15$ are marked with circles and triangles, respectively. The total energy of the wave packet is about one third of the barrier height. Time is shown in atomic units scaled by mass $\mu = 918m_e$.

cedure can be repeated in the course of dynamics, updating the mixed representation as the new minima or other linearizable features in the density develop. This strategy allows us to propagate arbitrary wave packets with a node or multiple nodes if it is combined with the LQF formulation on spatial domains.³¹

The mixed representation can also be viewed as a first correction to a Gaussian wave function in an anharmonic system. As an illustration we consider scattering of a low-energy Gaussian wave packet on the Eckart barrier representing the transition state of the H_3 system. In atomic units scaled by the reduced mass of hydrogen $\mu = 918m_e$ the potential V is given by $V = D \cosh^{-2}(\gamma x)$ with the parameter values $D = 16.0$ and $\gamma = 1.3624$. The mass is $m = 1$, the unit of energy is $[\text{hartree}] \times \mu$, the unit of time is $[\text{a.u.}] \times \mu^{-1}$. The initial wave packet is a Gaussian, $\psi(x,0) = (2\alpha/\pi)^{1/4} \exp[-\alpha(x-x_0)^2 + ip_0(x-x_0)]$, with a set of parameters $\{\alpha = 2.0, x_0 = -3.0, p_0 = 3.0\}$. The total energy of the wave packet is approximately equal to the one third of the barrier height. The wave packet transmission probabilities as a function of time are shown on Fig. 3. In the classical limit of the quantum potential being zero, the transmission probability is zero, since the classical energy of all the trajectories is less than the barrier height. The LQF method underestimates the transmission probability by a factor of 3: the approximate quantum potential redistributes the quantum potential energy between the trajectories reflecting the fact that the wave packet has low-amplitude components of the energy eigenstates with energies higher than the barrier height. Introduction of $\chi(x,t)$ at $t=0.1$, labeled $N=1$ on the figure, and an additional reexpansion at $t=0.15$, labeled $N=2$, improves the agreement with the quantum result describing tunneling due to the dynamical changes in the wave function density.

IV. CONCLUSIONS

We presented an approach to the description of the interference and the wave function nodes in the context of quantum trajectories. The approach is based on the mixed

coordinate/polar representation of the wave function. The modified trajectories governed by the polar part of the wave function give an efficient representation of the overall dynamics, while the coordinate space part $\chi(x,t)$ describes the interference features of the wave function density. This mixed description avoids the problems associated with the instability of the quantum trajectories and with the singularities of the quantum potential at the nodes of the wave function. At the same time the mixed description incorporates the feature of the quantum trajectories being the “ultimate” moving grid for the wave function.

In the context of semiclassical dynamics with the approximate quantum potential applicable to large systems, we also presented an approximate way of defining the coordinate space part of the wave function. All parameters in this model are found analytically from the moments of the position and momentum distributions, except for zero of $\chi(x,t)$ in the complex plane. The wave function normalization remains strictly conserved. The energy is not formally conserved, most likely due to the averaging procedure of obtaining time-dependent trajectory weights. Further improvements of the approximation and reexpansion methods are desirable and are currently under investigation. In particular, the multidimensional generalization of the method is conceptually straightforward, but its implementation requires multidimensional nonlinear optimization with respect to a complex vector instead of a single parameter z of Eq. (20) and will be presented in a future publication. (Generalization of the linear function $g(x)$ of Eq. (20) is completely analogous to the multidimensional version of the LQF method³⁰ and leads to a linear optimization problem.) Combination of the method with the LQF defined on spatial domains³¹ can describe multiple local features of the wave function.

As a concept, the mixed wave function representation allows one to balance the efforts between the polar representation, which is very efficient for diffuse structureless wave functions, and the coordinate space representation, which is better suited for description of the localized features of the wave function. The resulting trajectory dynamics is driven by the overall time evolution of the wave function providing a compact description in terms of trajectories. The dynamics can be made smooth and free of singularities making it computationally cheap. Local features due to quantum-mechanical interference or due to the initial form of a wave

function, that would require tight fixed grids, are describable in coordinate space in terms of $\chi(x,t)$. We believe, that this flexibility will give a better description of the interference and tunneling effects within the semiclassical dynamics in an efficient manner.

ACKNOWLEDGMENTS

Acknowledgment is made to the Donors of the American Chemical Society Petroleum Research Fund, for support of this research. This work was also supported by the NSF/EPSCOR under Grant No. EPS-0296165.

- ¹D. Bohm, Phys. Rev. **85**, 166 (1952).
- ²S. Garashchuk and V. A. Rassolov, Chem. Phys. Lett. **364**, 562 (2002).
- ³P. R. Holland, *The Quantum Theory of Motion* (Cambridge University Press, Cambridge, 1993).
- ⁴A. S. Sanz, F. Borondo, and S. Miret-Artes, J. Phys. I **14**, 6109 (2002).
- ⁵R. E. Wyatt, C. L. Lobreore, and G. Parlant, J. Chem. Phys. **114**, 5113 (2001).
- ⁶E. Gindensperger, C. Meier, and J. A. Beswick, J. Chem. Phys. **113**, 9369 (2000).
- ⁷I. Burghardt and L. S. Cederbaum, J. Chem. Phys. **115**, 10303 (2001).
- ⁸I. Burghardt and L. S. Cederbaum, J. Chem. Phys. **115**, 10312 (2001).
- ⁹I. Burghardt and K. B. Moller, J. Chem. Phys. **117**, 7409 (2002).
- ¹⁰J. B. Maddox and E. R. Bittner, J. Phys. Chem. B **106**, 7981 (2002).
- ¹¹E. R. Bittner, J. B. Maddox, and I. Burghardt, Int. J. Quantum Chem. **89**, 313 (2002).
- ¹²A. Donoso and C. C. Martens, Phys. Rev. Lett. **87**, 223202 (2001).
- ¹³C. J. Trahan and R. E. Wyatt, J. Chem. Phys. **119**, 7017 (2003).
- ¹⁴B. K. Dey, A. Askar, and H. Rabitz, J. Chem. Phys. **109**, 8770 (1998).
- ¹⁵C. L. Lobreore and R. E. Wyatt, Phys. Rev. Lett. **82**, 5190 (1999).
- ¹⁶D. Nerukh and J. H. Frederick, Chem. Phys. Lett. **332**, 145 (2000).
- ¹⁷E. R. Bittner and R. E. Wyatt, J. Chem. Phys. **113**, 8888 (2000).
- ¹⁸R. E. Wyatt and K. Na, Phys. Rev. E **65**, 016702 (2002).
- ¹⁹E. R. Bittner, J. Chem. Phys. **112**, 9703 (2000).
- ²⁰R. E. Wyatt and E. R. Bittner, J. Chem. Phys. **113**, 8898 (2000).
- ²¹B. K. Kendrick, J. Chem. Phys. **119**, 5805 (2003).
- ²²R. E. Wyatt, CNLS Workshop: Quantum and Semiclassical Molecular Dynamics of Nanostructures, 2004.
- ²³W. Poirier, CNLS Workshop: Quantum and Semiclassical Molecular Dynamics of Nanostructures, 2004.
- ²⁴C. J. Trahan, K. Hughes, and R. E. Wyatt, J. Chem. Phys. **118**, 9911 (2003).
- ²⁵J. Liu and N. Makri, J. Phys. Chem. A **108**, 5408 (2004).
- ²⁶S. Garashchuk and V. A. Rassolov, J. Chem. Phys. **118**, 2482 (2003).
- ²⁷S. Garashchuk and V. A. Rassolov, Chem. Phys. Lett. **376**, 358 (2003).
- ²⁸S. Garashchuk and V. A. Rassolov, Int. J. Quantum Chem. **99** (2004).
- ²⁹G. D. Billing, J. Chem. Phys. **110**, 5526 (1999).
- ³⁰S. Garashchuk and V. A. Rassolov, J. Chem. Phys. **120**, 1181 (2004).
- ³¹V. A. Rassolov and S. Garashchuk, J. Chem. Phys. **120**, 6815 (2004).